Rocklogger – can a smartphone replace a geological compass?

Bachelor thesis

Lehrstuhl für Geologie und Lagerstättenlehre

Montanuniversität Leoben

Timotheus Steiner

Abstract

The possibility of using a smartphone with the app “Rocklogger” instead of a geological compass was examined. For this purpose, around 350 pairs of geological measurements, each carried out by a geological compass and a smartphone, were collected. These values were compared by their means and by vector subtraction. In direct comparison the digital data has a lower precision with a median deviation of 13°. There are of course also deviations at the mean values, but they are in most cases acceptable and the deviations get smaller, if there are more measurements. Therefore, smartphones can be used as geological compass, if some extra measurements are taken to compensate for the lower precision.

Zusammenfassung

Die Verwendbarkeit eines Smartphones mit der App „Rocklogger“ als geologischer Kompass wurde untersucht. Dafür wurden 350 Paare von Messwerten sowohl mit dem Geologenkompass als auch mit dem Smartphone gemessen und paarweise sowie über ihre Mittelwerte verglichen. Beim direkten Vergleich zeigte sich, dass die Präzision der digitalen Messungen schlechter als bei einem Geologenkompass ist, der Median der Abweichungen liegt bei 13°. Die Mittelwerte zeigten auch Abweichungen, allerdings waren diese in den meisten Fällen wesentlich geringer als bei den Einzelmessungen. Zudem stieg die Übereinstimmung der Mittelwerte mit der Anzahl der Messungen. Deswegen kann geschlussfolgert werden, dass moderne Smartphones als Geologenkompass verwendet werden können allerdings ist dabei zu beachten, dass zum Ausgleich der geringeren Präzision etwas mehr Messungen als mit einem Geologenkompass durchgeführt werden sollten.

Table of Contents

1 Introduction

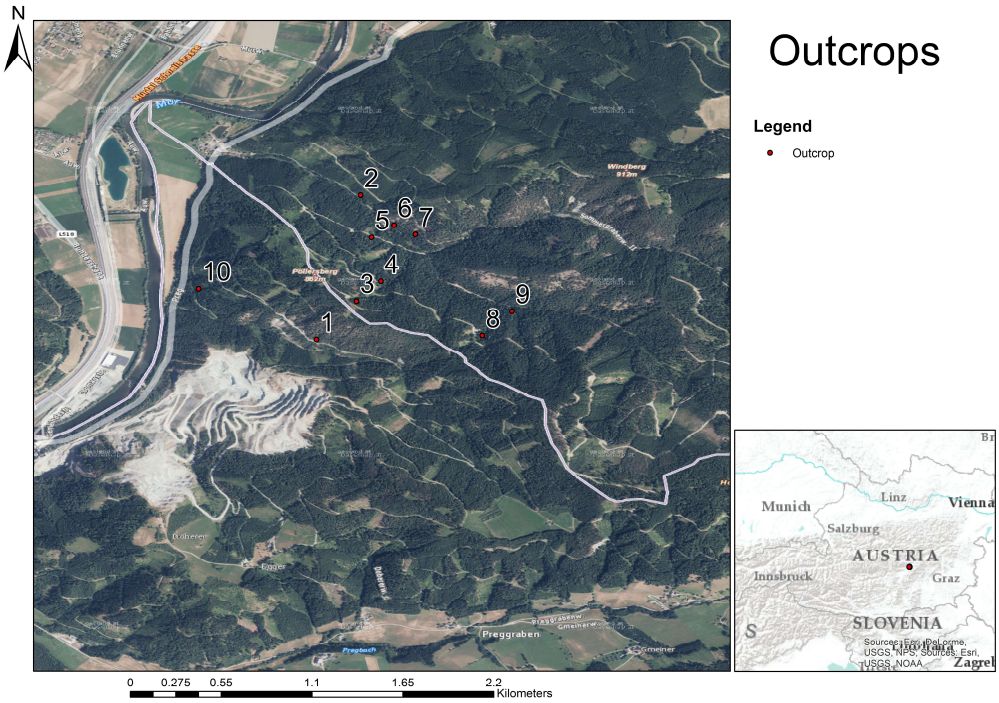

Figure 1: Map of the study area

Modern smartphones are today´s swiss knifes. It is not only possible to make phone calls, but one can also access the internet, make photos and do many things more. Since many modern smartphones have a dip sensor and a digital compass built in, it is theoretically possible to use them as geological compass. In fact, there are some applications, which are designed to do that. In this work “Rocklogger” is assessed in the area of Kraubath, the surveyed outcrops are shown in Figure 1. In contrast to a geological compass it records not only dip angle and dip direction, but also GPS coordinates, lithology (if given by the user), photos of the outcrops (if given by the user) and some more features and exports the data in a comma separated table (.csv format). The photos are referenced by their geographical positions and their file names. The measuring itself is faster and can be carried out at difficult positions like overhead in a mine. Thus, this application promises to save time in the fieldwork and the following digitalizing process.

As the advantages are clearly known, the assessment of the disadvantages is the topic of this work. When using Rocklogger, it soon becomes obvious, that not exactly the same values are measured as by a geological compass. Since all instruments have measurement errors, this is neither surprising, nor necessarily a problem. The question is, and will be answered in this work, if the data are true, or if there is any kind of systematic or random error, that influences the data.

2 Geological overview

The working area is located in the area of Kraubath (Styria), where the Speik Complex, which is part of the Silvretta-Seckau nappe system, is exposed (Moser 2016). The Speik-complex is a highly metamorphosed and deformed ophiolite (Neubauer et al. 1989). Neubauer et al. (1989) distinguish the following lithologies and their protoliths within the Speik-complex:

- Olivine-rich serpentinites: metamorphic peridotites, as depleted mantle material
- Stripped ultramafic rocks and metagabbros: ultramafic cumulates, the lowest part of the magma chamber
- Garnet amphibolite with marble, serpentinite lenses and gabbroic plagioclase amphibolite: mafic cumulates, the upper part of the magma chamber
- Gneiss, garnet mica schist, garnet amphibolite, augen gneiss and plagioclase amphibolite: extrusives, it is thought, that the sheeted dike complex would also belong to this group, but no evidence for that has been discovered yet
- Siliceous marble and sulphide-bearing mica schist: metamorphic oceanic sediments

The ophiolite probably formed in the Late Precambrium to Early Cambrium during accretion at the northern margin of Gondwana (Faryad et al. 2002, Melcher et al. 2002).

The Speik-complex in the study area is divided into two parts by the Miocene Mur-Mürz fault, which traces along the Mur-valley (Neubauer 1988, Sachsenhofer et al. 2003).

Mining in the area lastet for at least 200 years. In the past magnesite and chromium were mined; today, there is hard rock mining for railway ballast and there are recent explorations for Ni (Thalhammer et al. 2010).

3 Methods

3.1 Study area

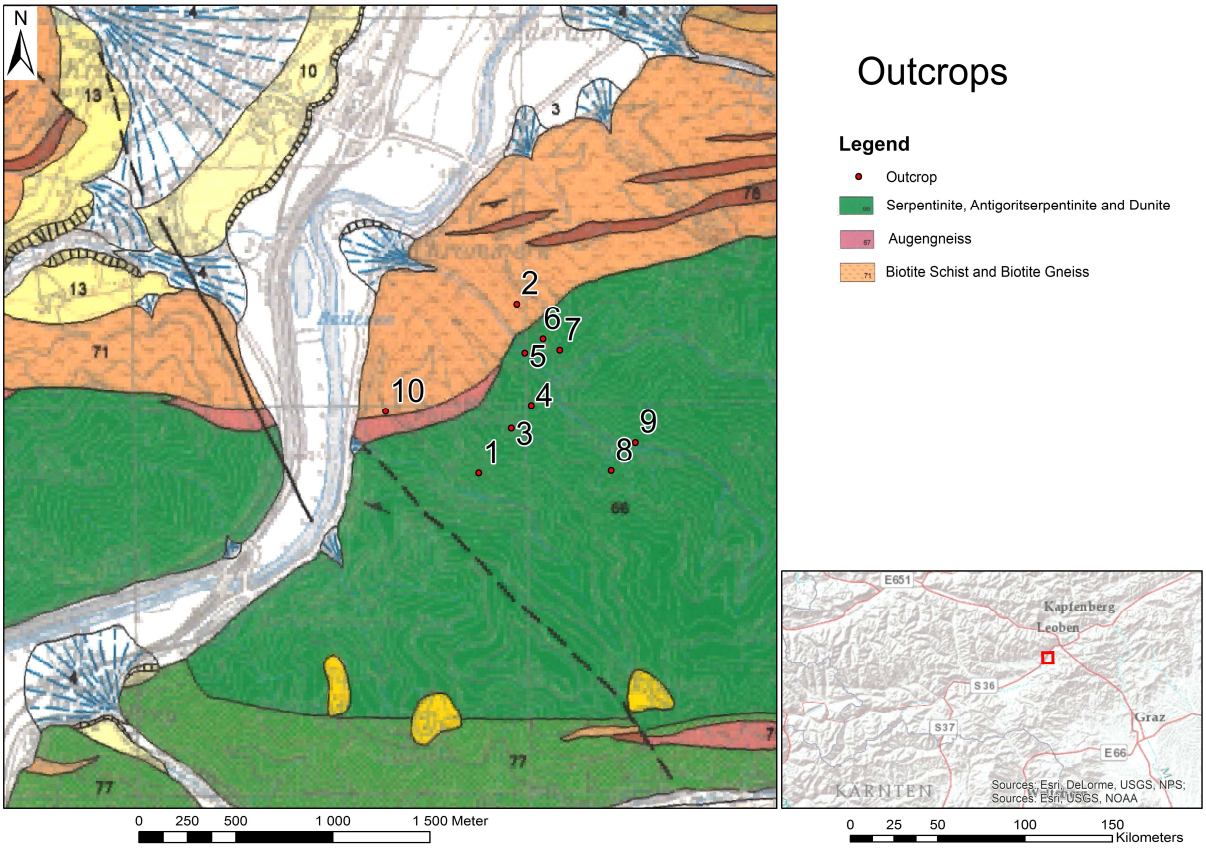

Figure 2: Geological map of the study area. The village in the upper left (in the area of the fan) is Kraubath/Mur. The Serpentinite and the Augengneiss are part of the Speik-complex, the Biotite Schists and Gneisses are metasediments of the Silvretta-Seckau nappe system. After Moser (2016)

The study area is located near Kraubath/Mur in Styria. All outcrops except outcrop 1 and outcrop 10 are in the "Wintergraben", a small valley S of Kraubath at Chromwerk. Outcrops 1 and 10 are located in the "Augraben". All outcrops are near to forest roads (Figure 2). The outcrops expose Serpentinite, Antigoritserpentinite and Dunite as well as Augengneiss as part of the Speik-complex. In the outcrops mainly serpentinite and sometimes magnesite were found, dunite was only found relictic. The Biotite Schist and Biotite Gneiss is also part of the Silvretta-Seckau nappe system.

3.2 Rocklogger

For dip measurements, a geological compass and a smartphone were used. The smartphone is a "Samsung Galaxy K Zoom"; and the program used for the measurements is Rocklogger (Turner-Jones 2016), available at the Google Play Store for free and in a paid version, which takes measurements faster.

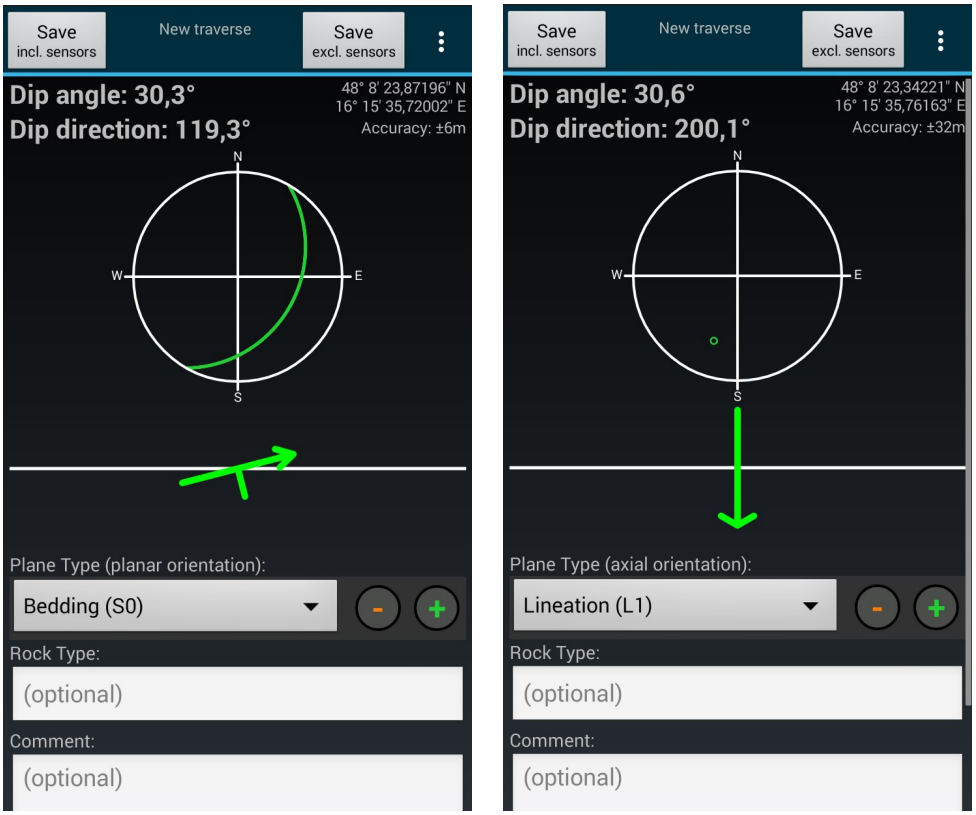

Figure 3: User interface of Rocklogger: (left) in plane recording mode; (right) in linear recording mode.

Before starting the measurements, it is necessary to calibrate the compass of the used smartphone. To do this, tap the three points in the upper right of the display in recording mode. Next, tap settings in the pop-up, scroll down to “Sensor calibration” in the settings and tap this. Then a window like in Figure 4 appears. Follow the instructions to calibrate the compass until the value for “Compass accuracy” changes to “3”. To achieve this, it is best to roll and tilt the smartphone in all directions.

Figure 4: Calibration of Rocklogger

The actual process of measurement started by marking the position of the measurement with chalk. This procedure assures, that exactly the same position is measured by both devices. The smartphone was aligned parallel to the inclination. After a few seconds the measurement was obtained by pressing the button “Save incl. sensors”. Figure 3 shows the user interface of Rocklogger.

3.3 Analysis

For plotting the acquired values the software OpenStereo (Grohmann and Campanha 2010) was used. For every dataset, all measurements of a plane with one method, the mean vector and the 95% confidence cone were calculated. This is only possible for datasets with more than 4 vectors (Braitsch 1956). A confidence cone is the cone, in which the true mean value is with a given probability (Braitsch 1956). If the compass data and the digital data are corresponding, they must plot in each other’s confidence cone. The following terminology will be used to describe the correspondence of mean vectors:

Very good correspondence: Mean vectors, that plot in each other’s confidence cone and are near to each other

Fair correspondence: Mean vectors, that plot in each other’s confidence cone or directly on the line of the confidence cone.

No correspondence: Mean vectors that do not share a common confidence cone.

In addition, the individual values were also compared pairwise. In the following, the used calculation method is described. Compass data can be interpreted as vectors in a spherical coordinate system. An easy way to determine the angle between two vectors in spherical coordinates is converting them into Cartesian coordinates. To calculate the angle between two planes, the angle between their pole points has to be calculated (Cardozo and Allmendinger 2013). Figure 5 illustrates the transformation.

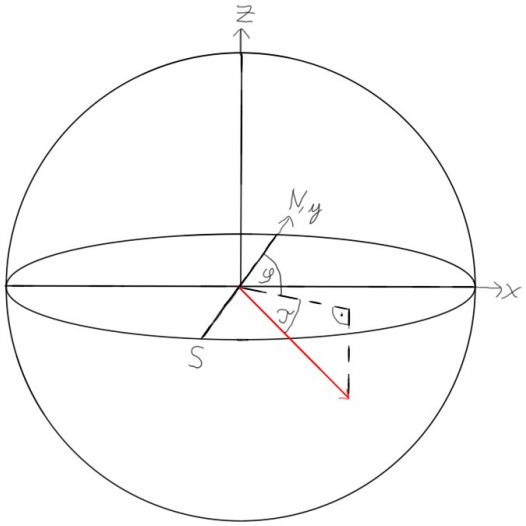

Figure 5: Converting compass data to a vector. N is the North direction; x,y,z are the coordinate axes; φ is the dip direction and τ is the dip.

Vectors in this coordinate system are estimated by Equation 1, where φ is the dip direction, τ is the dip and r is the distance to the coordinate origin. Since compass data have no length and r is needed for the calculations, r equals 1.

$$\vec{a} = \begin{pmatrix} \varphi \\ \tau \\ r \end{pmatrix}$$

Equation 1

The calculation follows Cardozo and Allmendinger (2013). The calculation was performed by Excel using radian as input for trigonometric functions. As next step the cosine of α, the angle between the two vectors $\vec{a}$ and $\vec{b}$ and hence geological planes, was calculated as in Equation 4. For this, it is necessary to derive the pole to the plane ($\vec{a}$) and then transform to Cartesian coordinates, this is shown in Equation 2.

$$\begin{pmatrix} \varphi \\ \tau \\ r \end{pmatrix} = \begin{pmatrix} \varphi \\ \tau \\ 1 \end{pmatrix} \rightarrow \begin{pmatrix} \varphi + 180 \\ 90 - \tau \\ 1 \end{pmatrix} = \vec{a} = \begin{pmatrix} \sin(\varphi_a) * \cos(\tau_a) \\ \cos(\varphi_a) * \cos(\tau_a) \\ -\sin(\tau_a) \end{pmatrix}$$

Equation 2

Next the cosine of the angle between the two vectors $\vec{a}$ and $\vec{b}$ is calculated in Equation 3. The length of both vectors is 1, therefore the numerator is 1 and the formula can be written as in Equation 4.

$$\cos\alpha = \frac{\vec{a} * \vec{b}}{|\vec{a}| * |\vec{b}|}$$

Equation 3

$$\cos\alpha = \sin(\varphi_a) * \cos(\tau_a) * \sin(\varphi_b) * \cos(\tau_b) + \cos(\varphi_a) * \cos(\tau_a) * \cos(\varphi_b) * \cos(\tau_b) + \sin(\tau_a) * \sin(\tau_b)$$

Equation 4

As last step α is calculated from its cosine (Equation 5) and converted back into degrees. The result is the angle between the two input planes.

$$\alpha = \cos^{-1}(\alpha)$$

Equation 5

Since vectors have a direction, the derived angle varies between 0° and 180°. This is not true for angles between planes, therefore, all angles greater than 90° are substracted from 180°.

4 Outcrops

Every plotted Schmidt net was labelled following the scheme outcrop_dataset, e.g. 1_sf stands for the schistosity plane in outcrop 1.

4.1 Outcrop 1

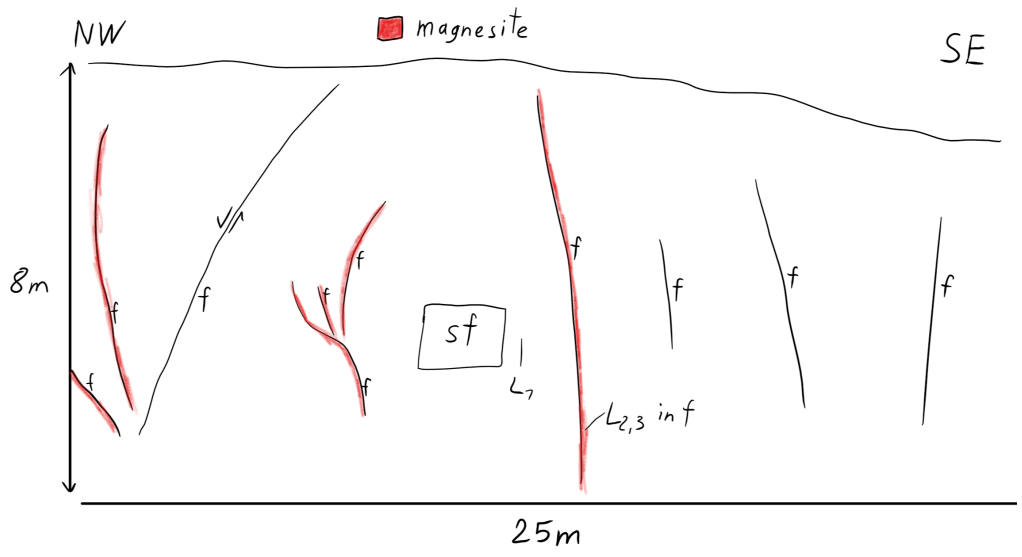

Figure 6: Sketch of outcrop 1. Abbreviations: f = fault, L = Lineation, sf = schistosity

Outcrop 1 is a huge outcrop along the forest road in the upper part of the Augraben of which the middle part was examined. The outcrop mainly consists of serpentinite bearing magnetite and some chromite. Unlike most other outcrops the dominating structures are faults. The faults

are steep and many of them host magnesite, see Figure 6. In the magnesite lineations can be seen, therefore it is likely, that the magnesite formed simultaneous with the faulting event.

Figure 7 shows the Schmidt nets for this outcrop. For the faults, there is a very good correspondence of the compass and digital data. The lineations generally show a large scatter for both methods, the mean values show a fair correspondence. At the schistosity planes the digital data are more scattered than the compass data and the mean values show no correspondence.

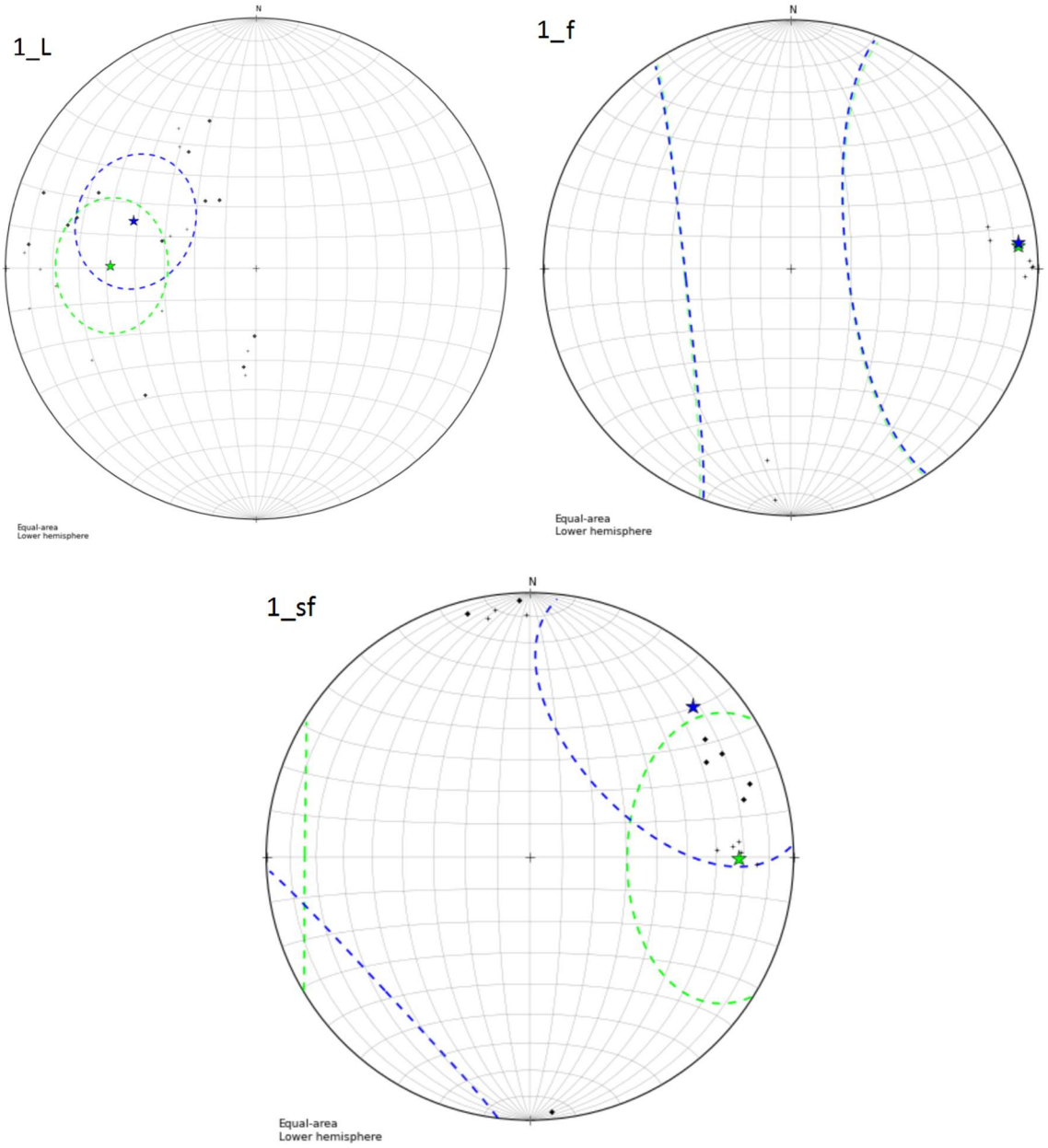

Figure 7: Schmidt nets of the structures of outcrop 1; 1_L: lineations; 1_f: faults; 1_sf: schistosity planes. Green star: mean value of the compass data; green small circle: 95% cone of the compass data; small crosses: compass data points; blue star: mean value of the digital data; blue small circle: 95% confidence cone of the digital data; black dots: digital data points.

4.2 Outcrop 2

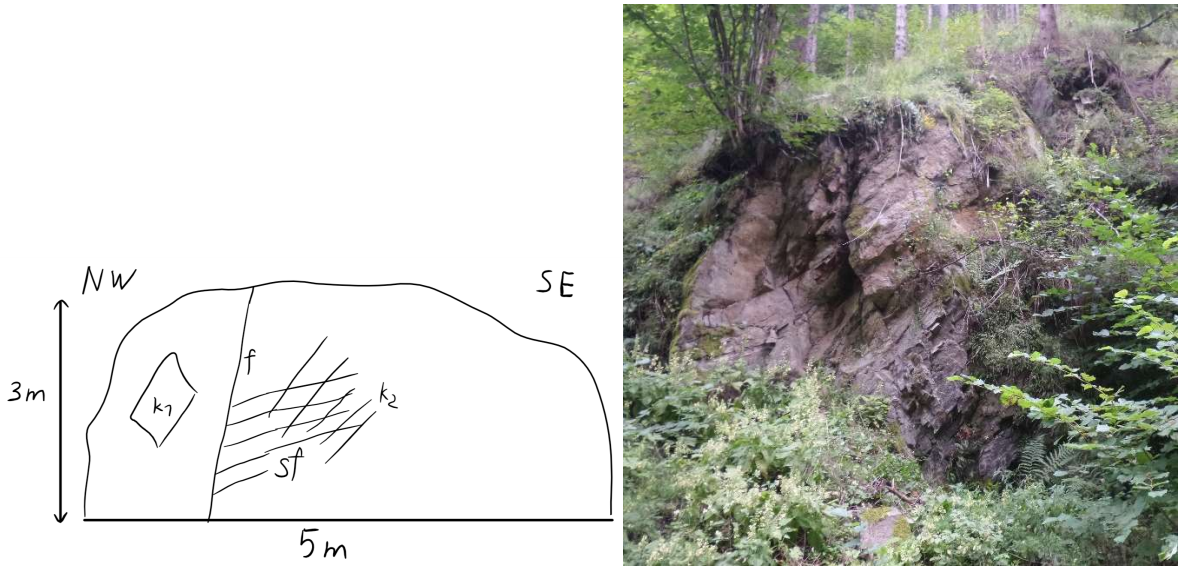

Figure 8: Sketch and a photo of outcrop 2. Abbreviations: f = fault, k= joint, sf = schistosity

Outcrop 2 is located in the Wintergraben along the forest road. It comprises foliated gneiss. In the fault there is a fine grained fault breccia.

Figure 9 shows the Schmidt nets of the structures. The mean values of the fault show a good correspondence. The mean values of the joints show no correspondence. The mean values of the schistosity show a large scatter and a fair correspondence.

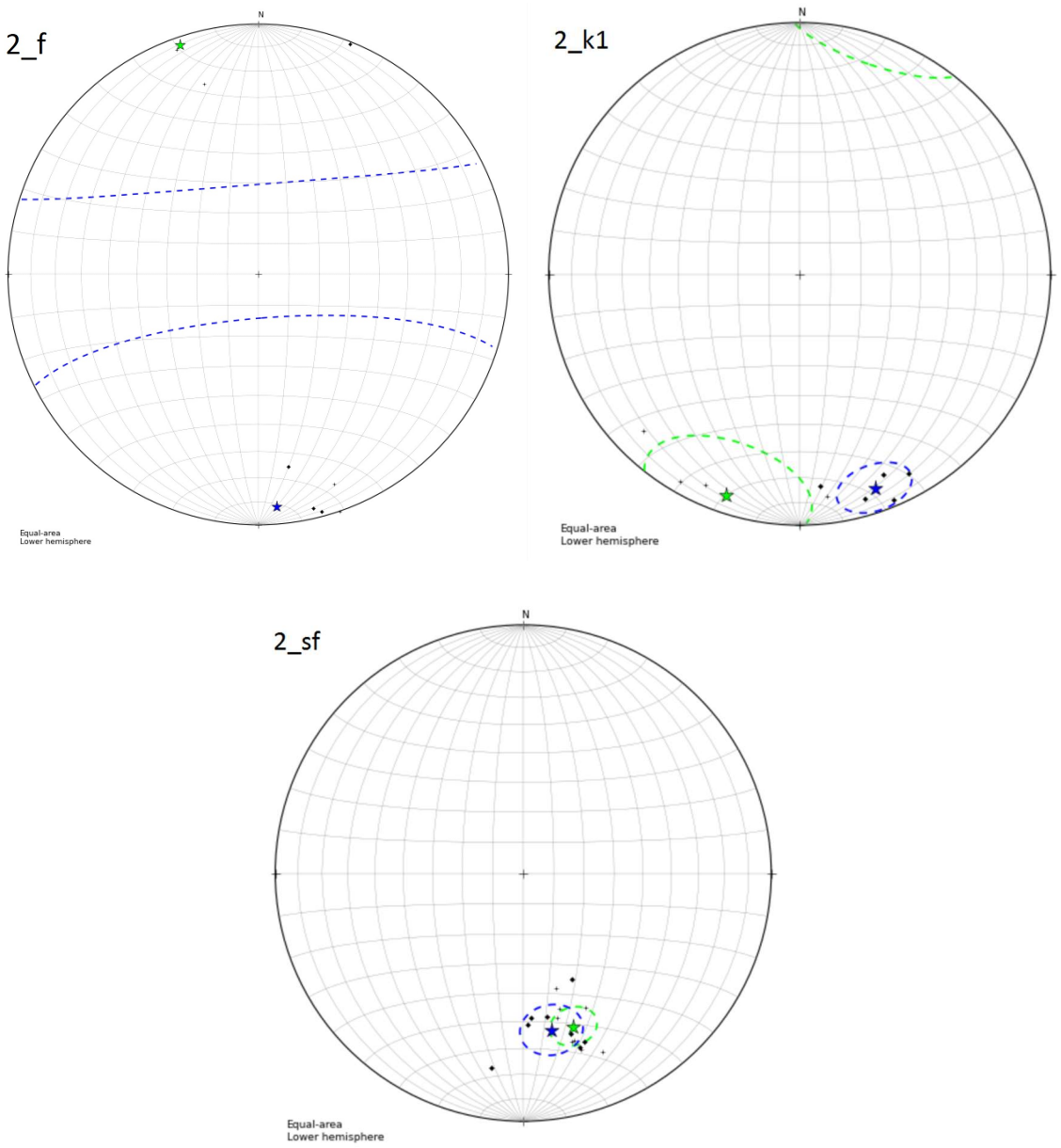

Figure 9: Schmidt nets of the structures of outcrop 2; 2_f: fault; 2_k1: jointset 1; 2_sf: schistosity planes. Green star: mean value of the compass data; green small circle: 95% cone of the compass data; small crosses: compass data points; blue star: mean value of the digital data; blue small circle: 95% confidence cone of the digital data; black dots: digital data points.

4.3 Outcrop 3

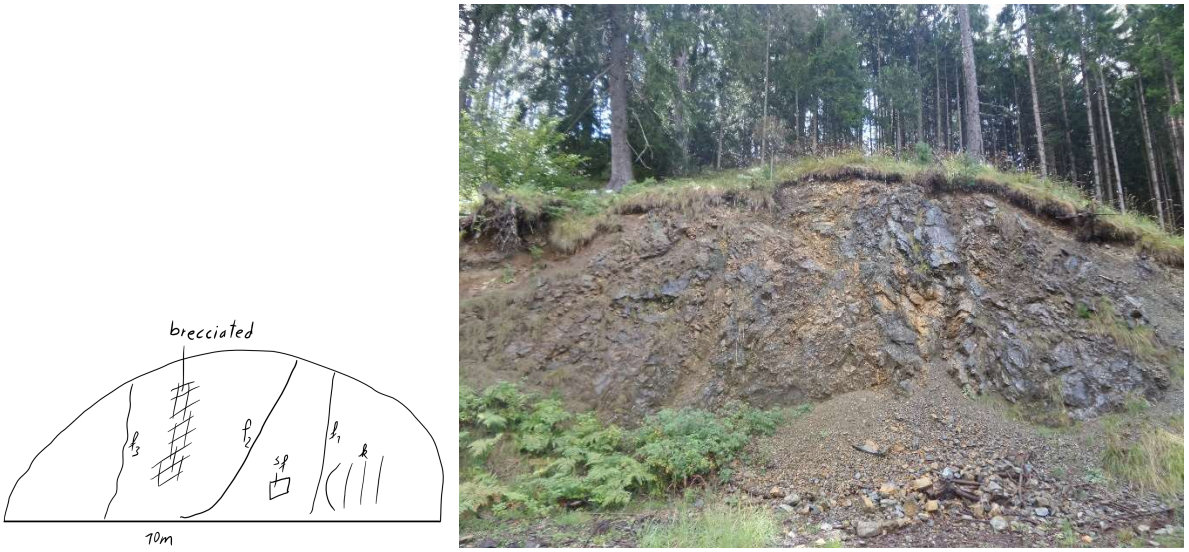

Figure 10:Sketch and a photo of outcrop 3. Abbreviations: f = fault, k= joint, sf = schistosity

Outcrop 3 is located near the ridge, bordering the Wintergraben to the S. It is composed of heavily weathered and brecciated serpentinite. Figure 10 shows the outcrop; the brecciated zone in the central part shows no evidence of a fault.

Figure 11 shows the Schmidt nets of the structures. For this outcrop all mean values show good correspondence and the data points show similar scattering.

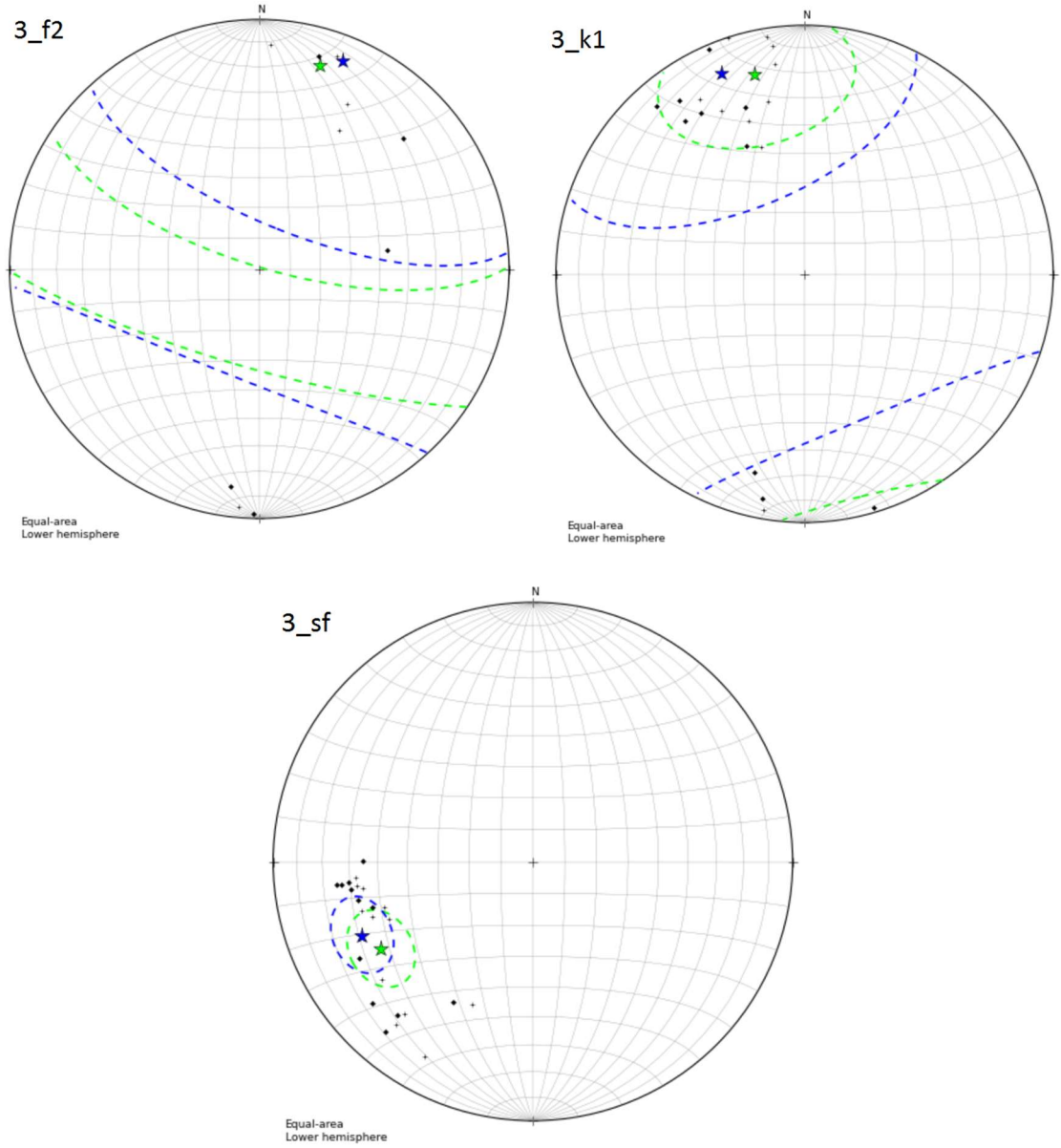

Figure 11: Schmidt nets of the structures of outcrop 3; 3_f: fault 2; 3_k1: jointset 1; 3_sf: schistosity planes. Green star: mean value of the compass data; green small circle: 95% cone of the compass data; small crosses: compass data points; blue star: mean value of the digital data; blue small circle: 95% confidence cone of the digital data; black dots: digital data points.

4.4 Outcrop 4

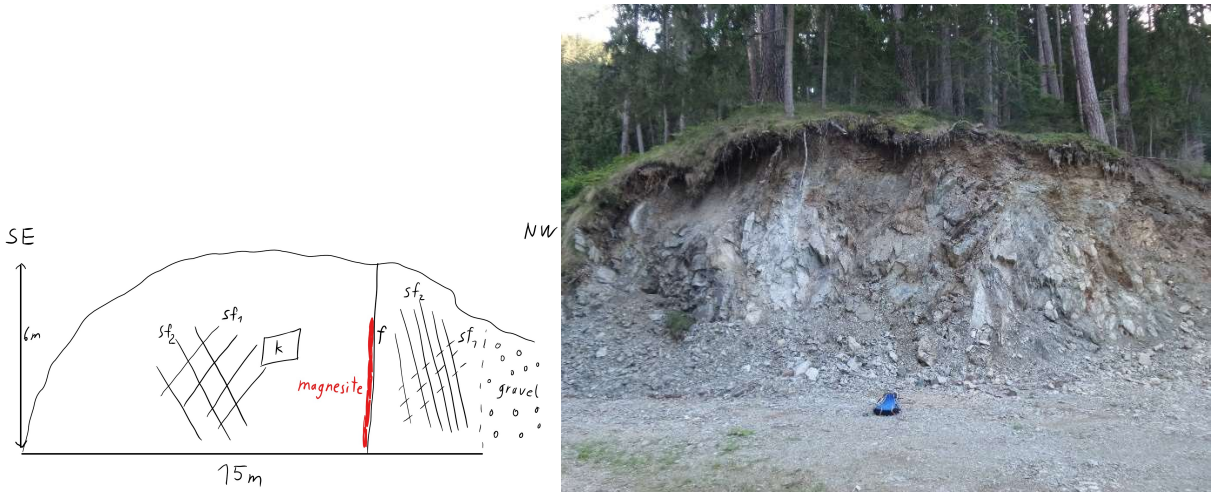

Figure 12:Sketch and a photo of outcrop 4. Abbreviations: f = fault, k= joint, sf = schistosity

Outcrop 4 is located 30 m lower than outcrop 3. It consists of serpentinite and magnesite in a large fault. Nearly the whole rock of the outcrop is broken to diamond-shaped pieces due to the two schistosity cleavages.

Figure 13 shows the Schmidt nets of the structures. All data points as well as the mean values show a very good correspondence. The scattering of the data points of the joints seems to indicate a tilt of the joint direction, maybe due to faulting.

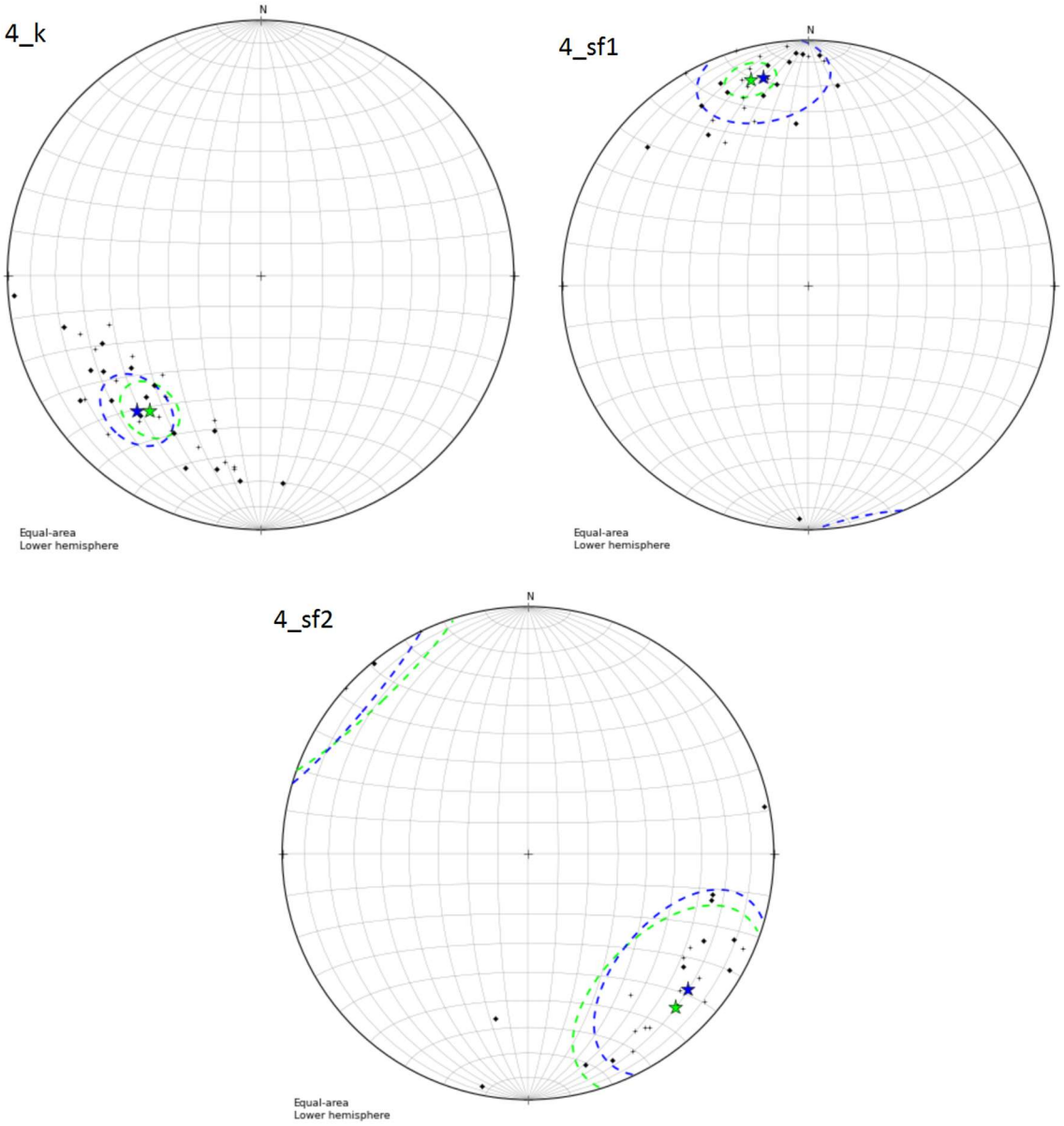

Figure 13: Schmidt nets of the structures of outcrop 4;4_k: joints; 4_sf1: schistosity 1; 4_sf2: schistosity 2. Green star: mean value of the compass data; green small circle: 95% cone of the compass data; small crosses: compass data points; blue star: mean value of the digital data; blue small circle: 95% confidence cone of the digital data; black dots: digital data points.

4.5 Outcrop 5

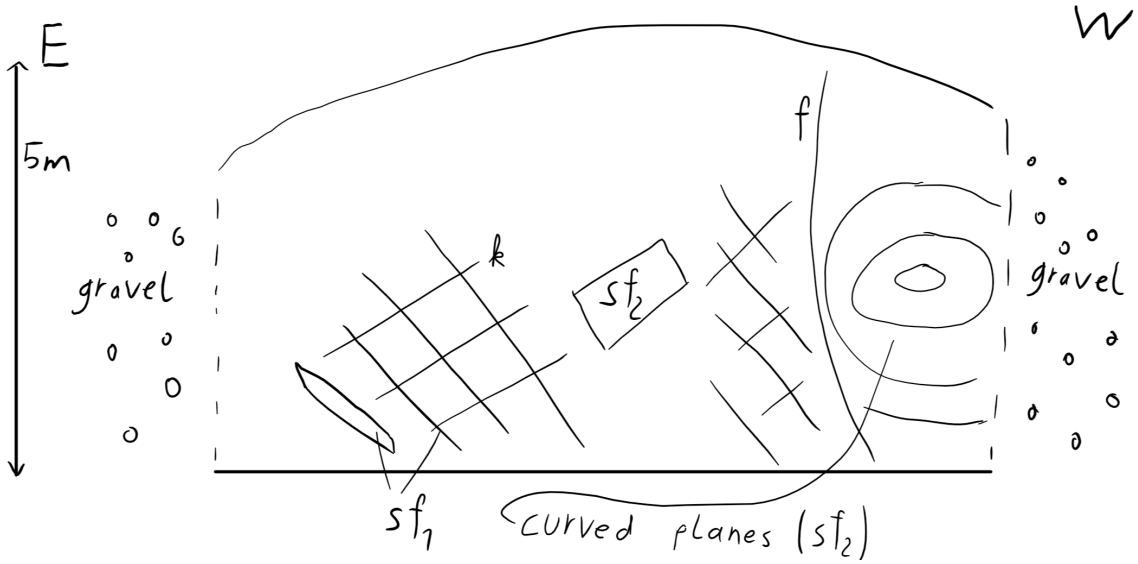

Figure 14: Sketch of outcrop 5. Abbreviations: f = fault, k= joint, sf = schistosity

Outcrop 5 is located at the forest road to outcrops 3 and 4 some 200 m after the confluence of the two creeks. Figure 14 shows the outcrop, the structures in the right part are similar to those found in the left part of outcrop 6. It is possible, that these structures represent pillows. The outcrop consists of serpentinite.

Figure 15 shows the Schmidt nets of the structures. The mean values of the data of the fault, the joints and the schistosity 2 show a very good correspondence and similar scattering. For the schistosity 1, the digital data shows a much larger scattering and the mean values show no correspondence.

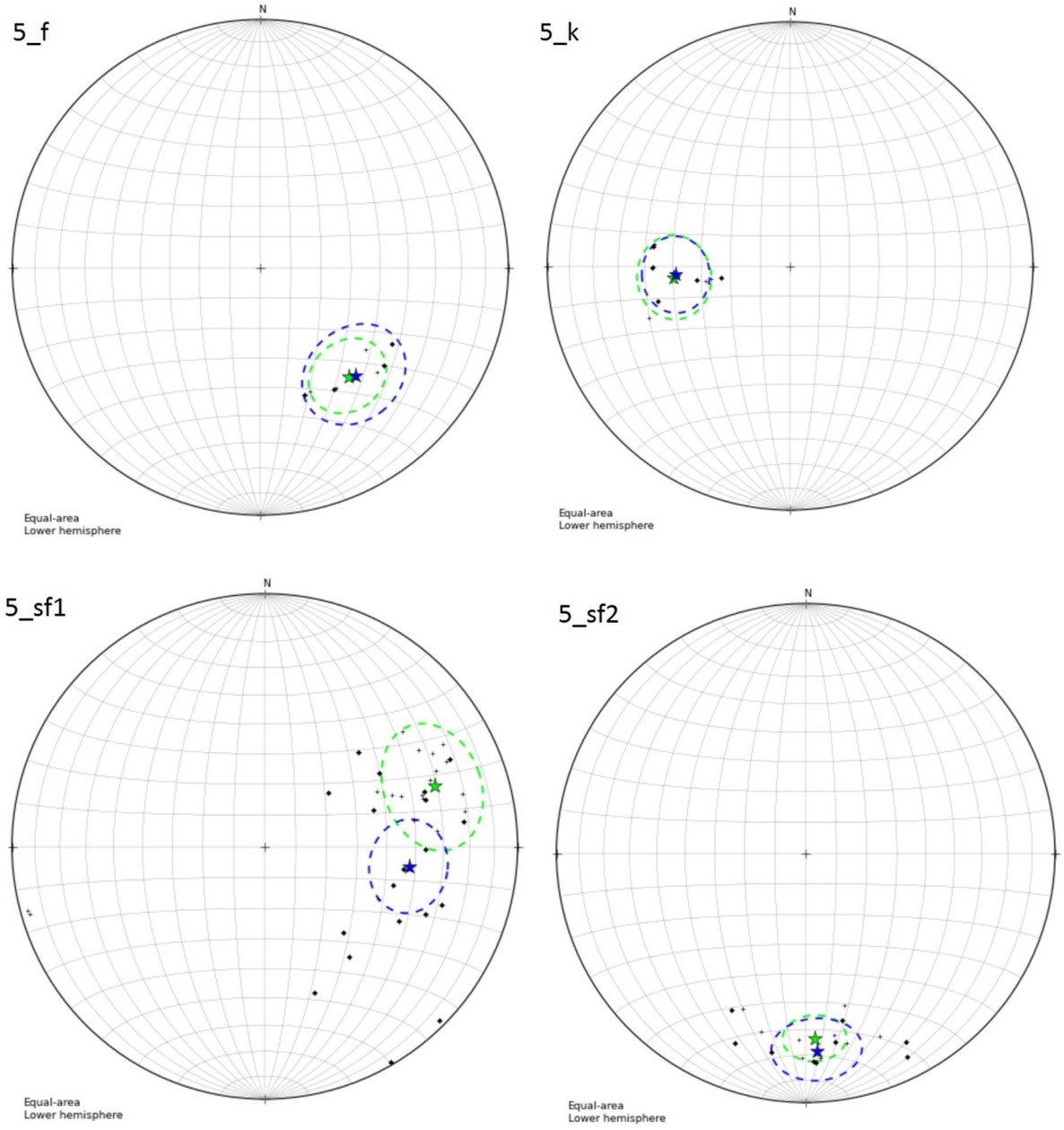

Figure 15: Schmidt nets of the structures of outcrop 5; 5_f: fault; 5_k: joints 1; 5_sf1: schistosity 1; 5_sf2: schistosity 2. Green star: mean value of the compass data; green small circle: 95% cone of the compass data; small crosses: compass data points; blue star: mean value of the digital data; blue small circle: 95% confidence cone of the digital data; black dots: digital data points.

4.6 Outcrop 6

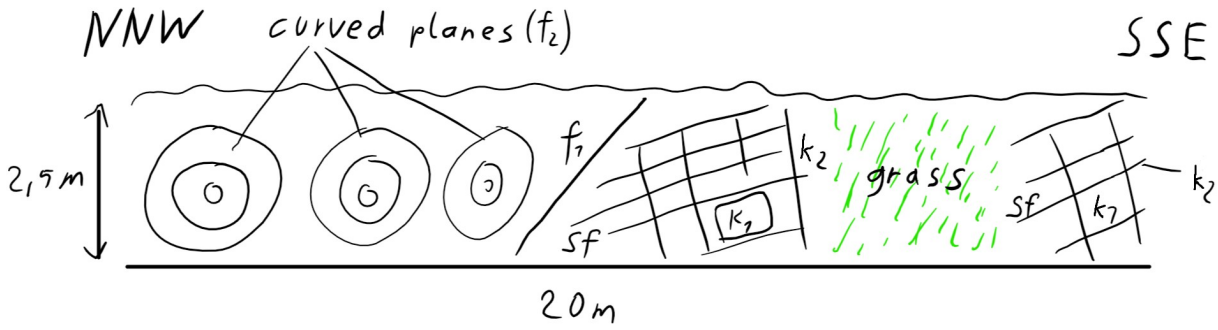

Figure 16: Sketch of outcrop 6. Abbreviations: f = fault, k= joint, sf = schistosity

Outcrop 6 is located in the lower part of the Wintergraben, 250m SE of outcrop 1. Figure 17 shows the left part of the outcrop; there are pillow-like bent surfaces. The round shapes are massive and have a 1cm thick crust (the greyish material in Figure 17). These observations suggest, that these structures are pillows. The whole outcrop consists of serpentinite.

Figure 17: Left part of outcrop 6, see Figure 16 for comparison.

Figure 18 shows the Schmidt nets of this outcrop. For the fault, the mean values show no correspondence. For joint set 1, the mean values show a fair correspondence, the same is true for joint set 2. For the schistosity, the mean values show a very good correspondence.

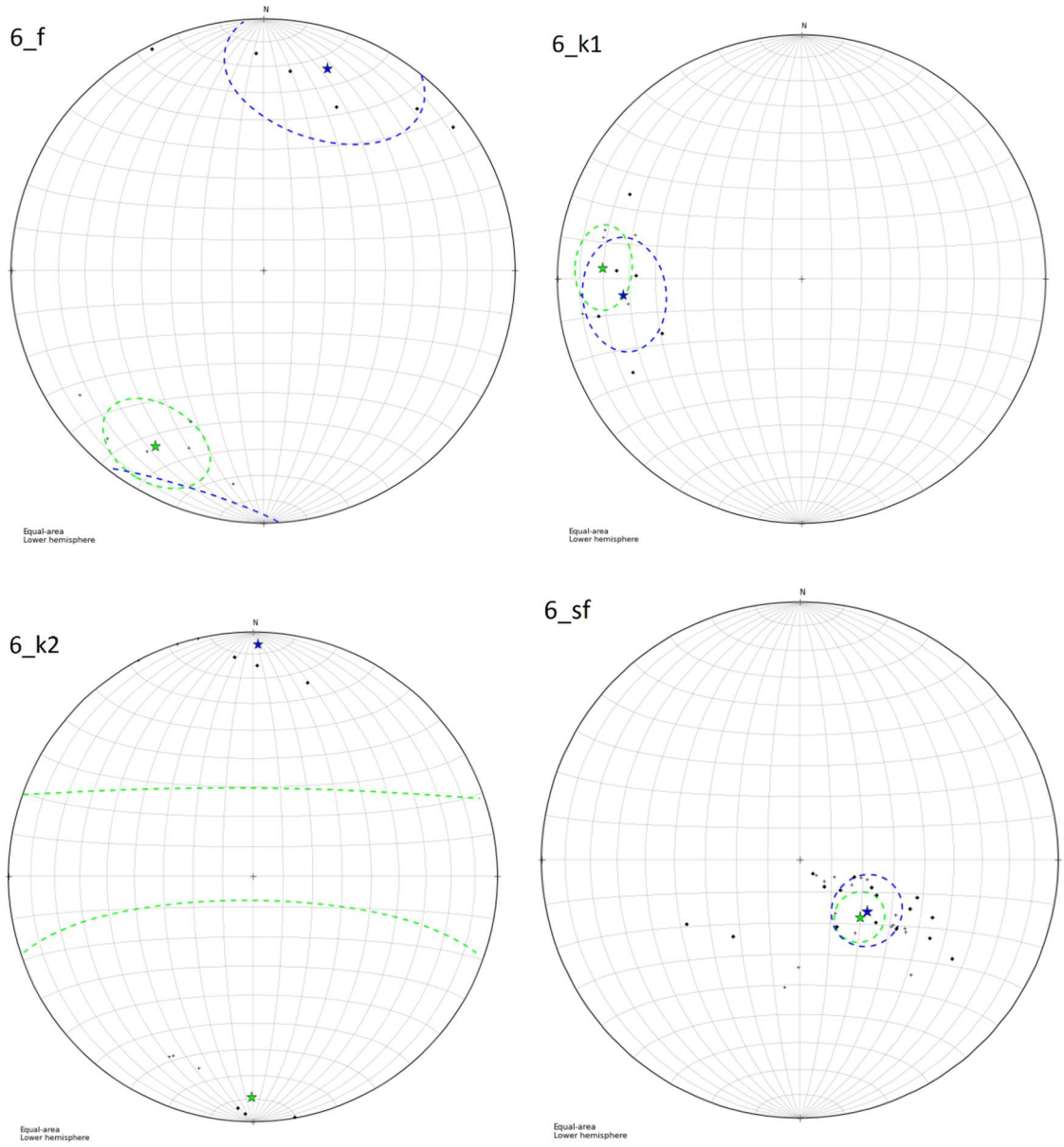

Figure 18: Schmidt nets of the structures of outcrop 6; 6_f: fault; 6_k1: joint set 1; 6_k2: joint set 2; 6_sf: schistosity. Green star: mean value of the compass data; green small circle: 95% cone of the compass data; small crosses: compass data points; blue star: mean value of the digital data; blue small circle: 95% confidence cone of the digital data; black dots: digital data points.

4.7 Outcrop 7

Figure 19: Sketch of outcrop 7. Abbreviations: f = fault, k= joint, L = Lineation, sf = schistosity

Outcrop 7 is located in the Wintergraben, 100 m from outcrop 6 to the southeast. As Figure 19 shows, this outcrop consists of two small outcrops. This outcrop consists of serpentinite.

Figure 20 shows the Schmidt nets of outcrop 7. The mean values of fault 1 and joint set 1 show a very good correspondence, although the data of the joints are very scattered. The mean values of joint set 2 and the schistosity show no correspondence, this is in both cases an effect of the scattering.

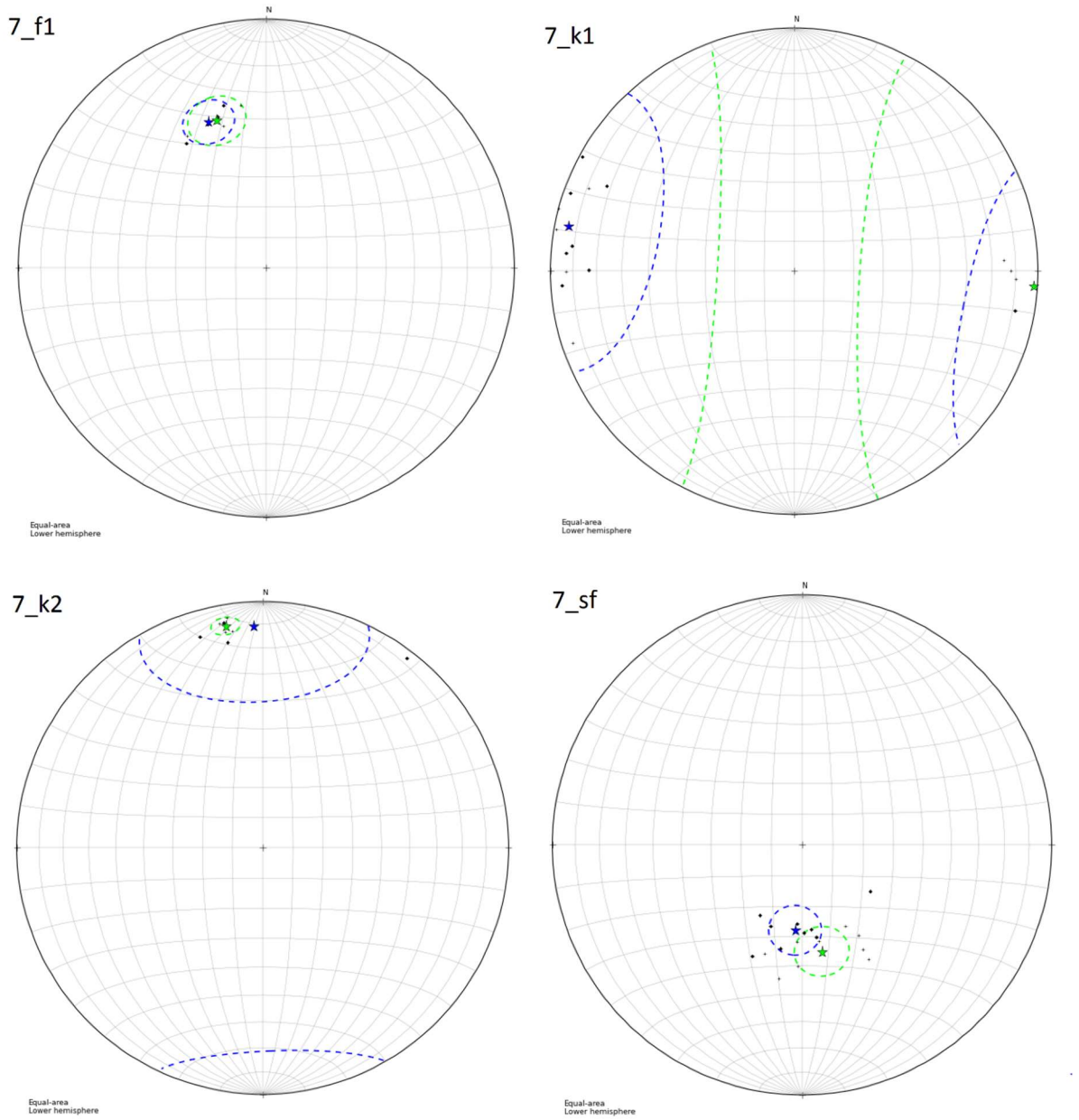

Figure 20: Schmidt nets of the structures of outcrop 7; 7_f1: fault 1; 7_k1: joint set 1; 7_k2: joint set 2; 7_sf: schistosity. Green star: mean value of the compass data; green small circle: 95% cone of the compass data; small crosses: compass data points; blue star: mean value of the digital data; blue small circle: 95% confidence cone of the digital data; black dots: digital data points.

4.8 Outcrop 8

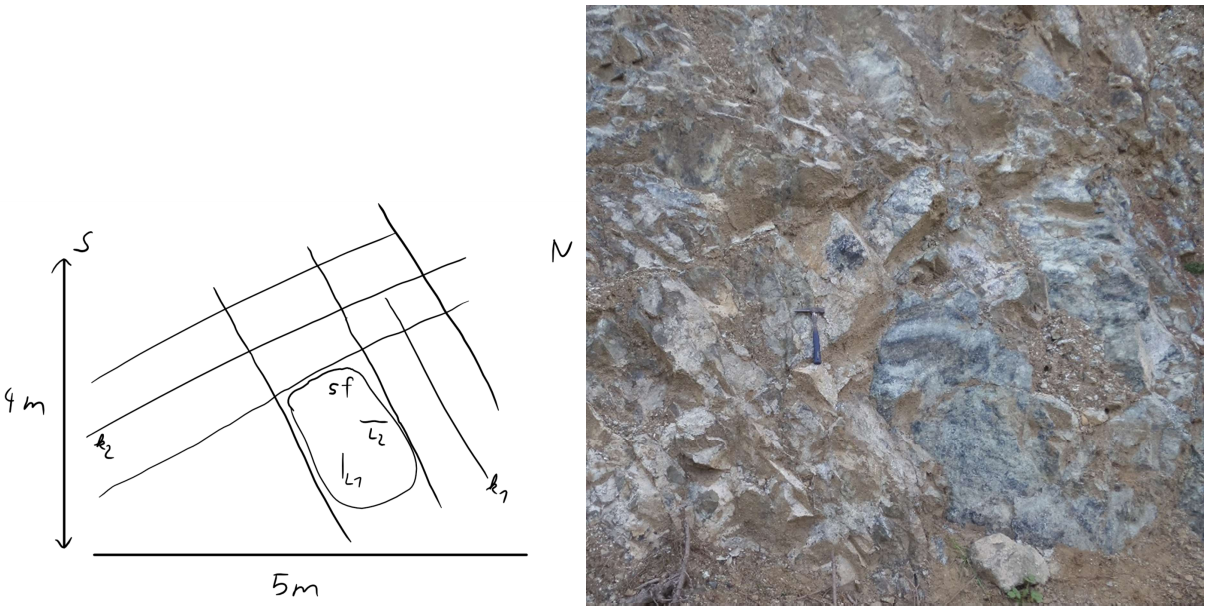

Figure 21: Sketch and a photo of outcrop 8. Abbreviations: k= joint, L = Lineation, sf = schistosity

Outcrop 8 is a huge outcrop, of which the lower central part was examined. The outcrop consists of serpentinite with magnesite bound to joints.

Figure 22 shows the Schmidt nets of this outcrop. The mean vectors of the lineations show a very good correspondence. The mean vectors of joint set 1 show fair correspondence and the mean vectors of joint set 2 show very good correspondence. The mean vectors of the schistosity data show fair correspondence.

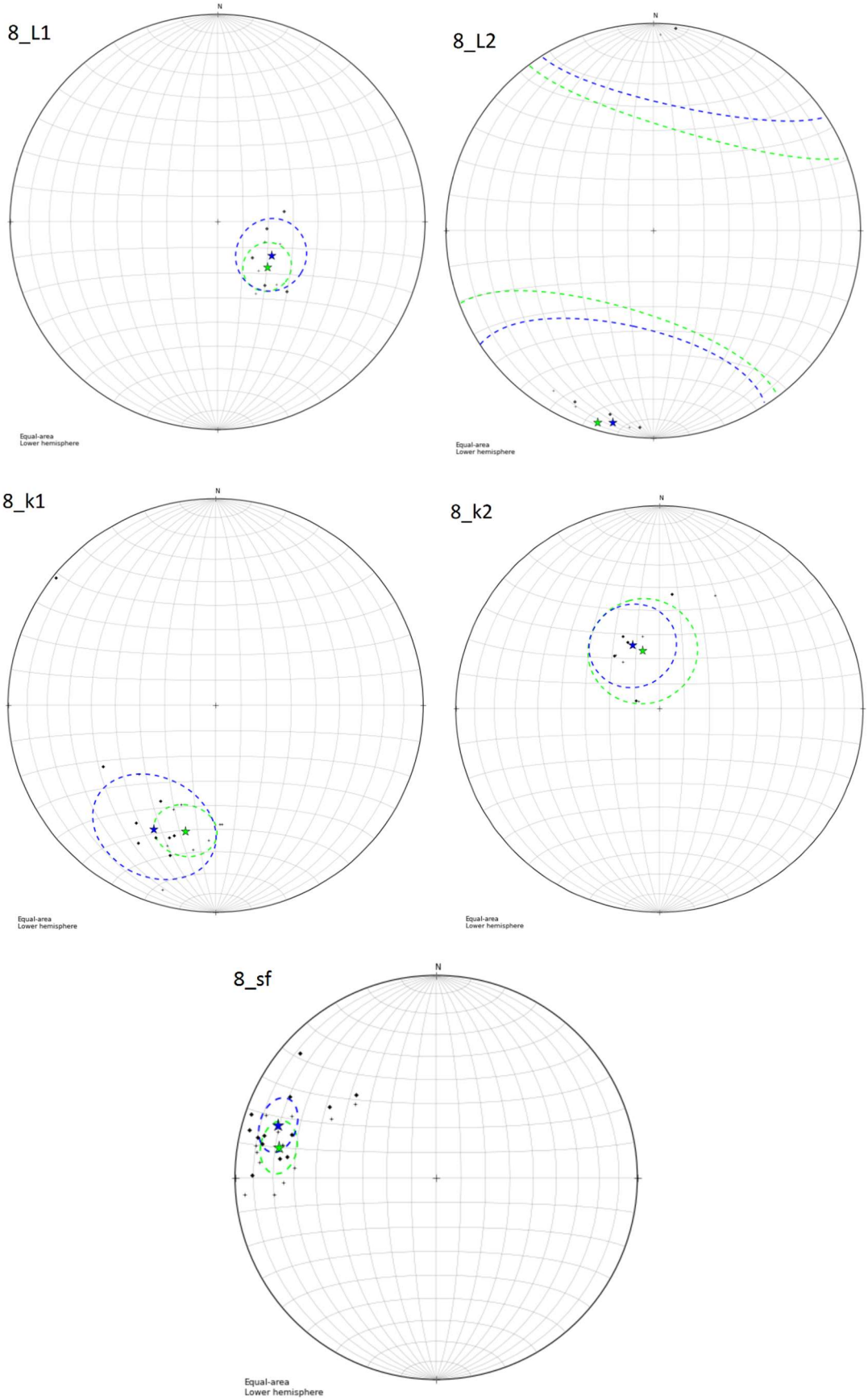

Figure 22: Schmidt nets of the structures of outcrop 8; 8_L1: Lineation set 1; 8_L2: Lineation set2; 8_k1: joint set 1; 8_k2: joint set 2;8_sf: schistosity. Green star: mean value of the compass data; green small circle: 95% cone of the compass data; small crosses: compass data points; blue star: mean value of the digital data; blue small circle: 95% confidence cone of the digital data; black dots: digital data points.

4.9 Outcrop 9

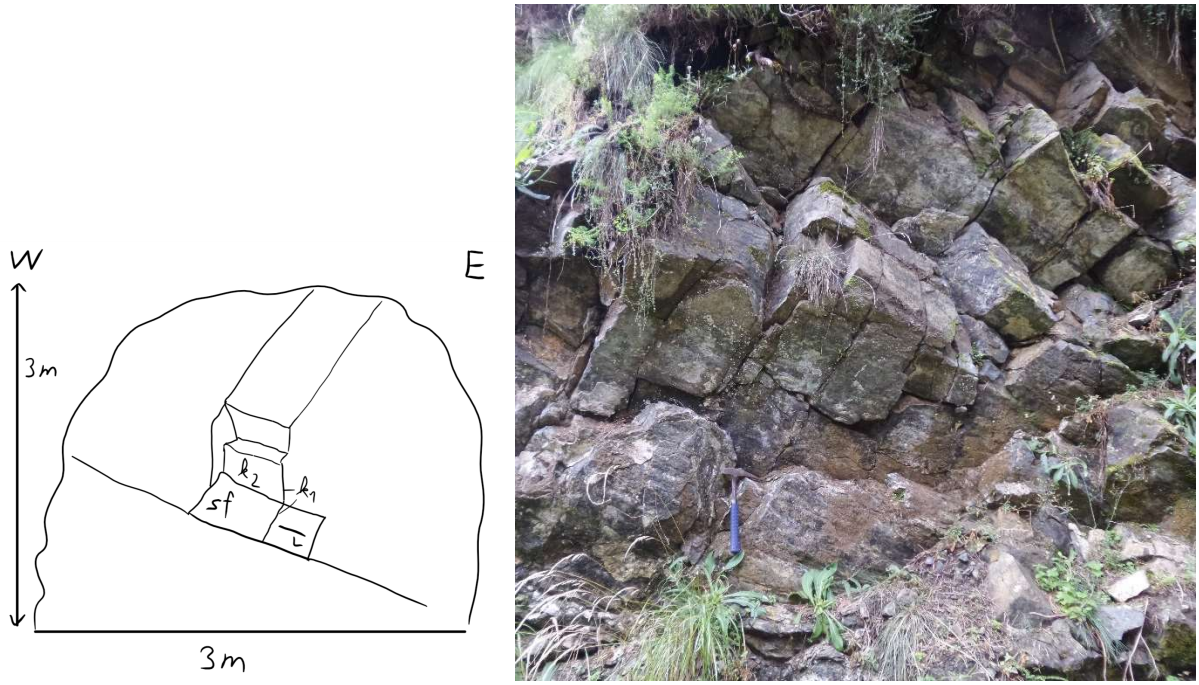

Figure 23: Sketch and a photo of outcrop 9. Abbreviations: k= joint, L = Lineation, sf = schistosity

Outcrop 9 is in the Wintergraben and consists of serpentinite.

Figure 24 shows the Schmidt nets of this outcrop. The Schmidt net of joint set 1 clearly shows two populations, one for each measurement method. This suggests a systematic error since it is very significant, the mean values show no correspondence. For joint set 2 and the schistosity, the mean values show fair correspondence, although it is again possible to distinguish two populations – one for each measurement method.

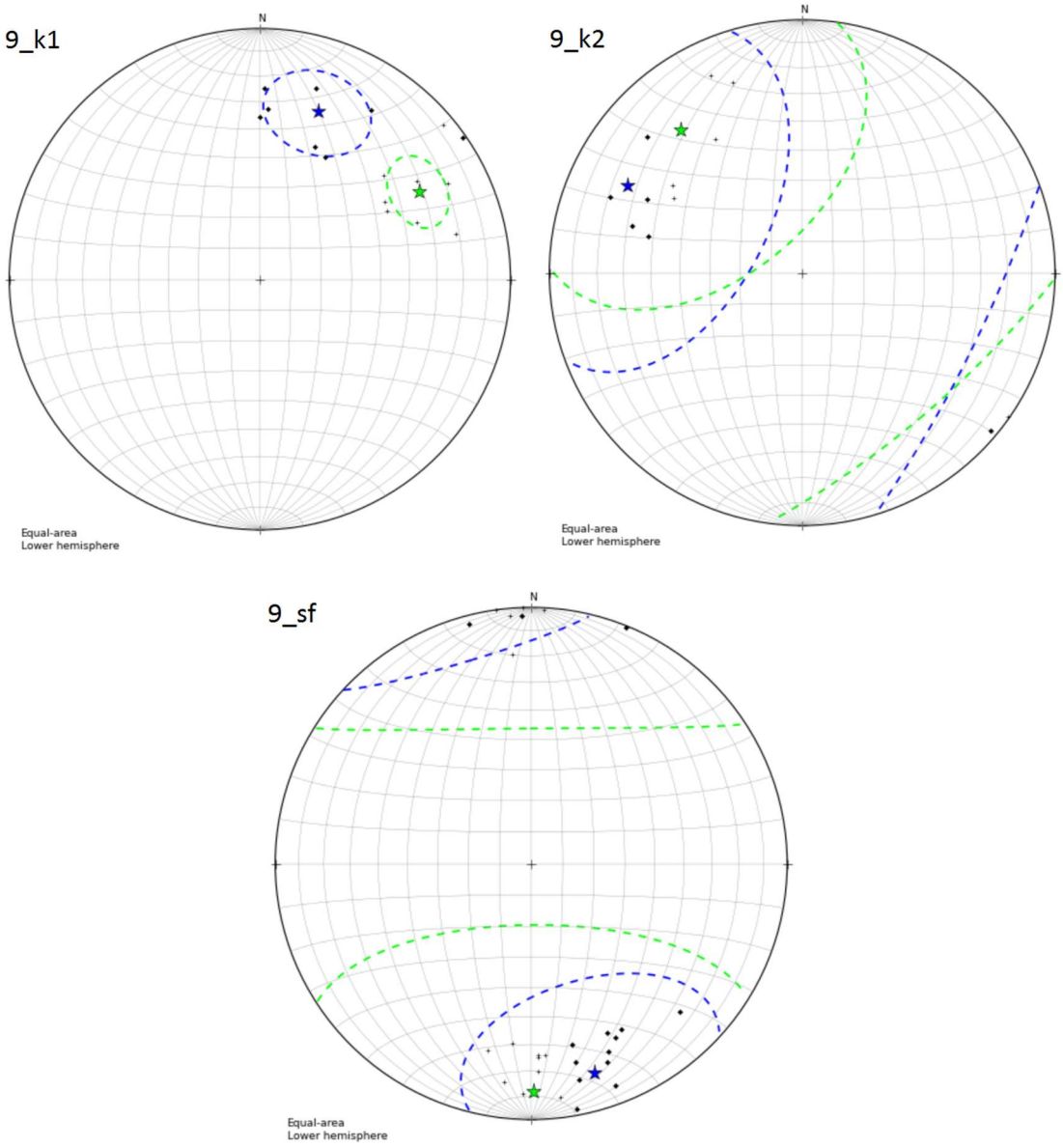

Figure 24: Schmidt nets of the structures of outcrop 9; 9k1: joint set 1; 9_k2: joint set 2;9_sf: schistosity. Green star: mean value of the compass data; green small circle: 95% cone of the compass data; small crosses: compass data points; blue star: mean value of the digital data; blue small circle: 95% confidence cone of the digital data; black dots: digital data points.

4.10 Outcrop 10

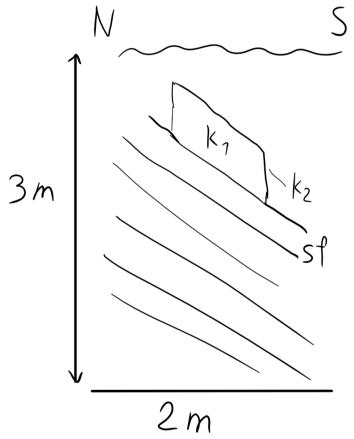

Figure 25: Sketch of outcrop 10. Abbreviations: k= joint, sf = schistosity

Outcrop 10 is in the Augraben. It stretches along the road for over 30 m. It consists of augengneiss. It should be noted, that in the geological map, this outcrop is not plotted within the area of augengneiss; the reason for this may be, that this geological map was created without additional mapping in the field and is only provisional (Moser 2016).

Figure 26 shows the Schmidt nets of this outcrop. The mean values of joint set 1 have a difference of over 70°. Interestingly, some of the digital data points plot in the area of the compass data. The mean vectors of the schistosity show very good correspondence.

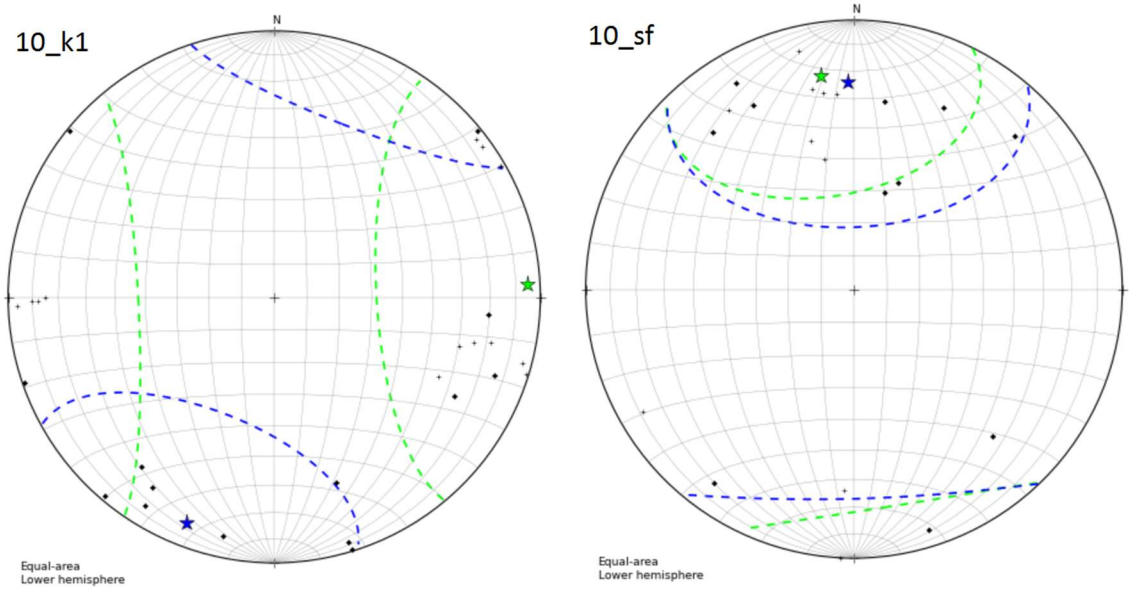

Figure 26: Schmidt nets of the structures of outcrop 10; 10k1: joint set 1; 10_sf: schistosity. Green star: mean value of the compass data; green small circle: 95% cone of the compass data; small crosses: compass data points; blue star: mean value of the digital data; blue small circle: 95% confidence cone of the digital data; black dots: digital data points.

5 Discussion

Since pairs of data – digital and compass data – were measured, it is possible to compare them pair by pair. Figure 27 shows a histogram with a sum curve of the deviations of the digital data from the compass data. 20% of the digital data show a deviation from the compass data smaller than 5°. 60% show a deviation smaller than 10° and 78% have a deviation smaller than 15°. This and a median of 13° suggests, that single digital measurements are not very precise.

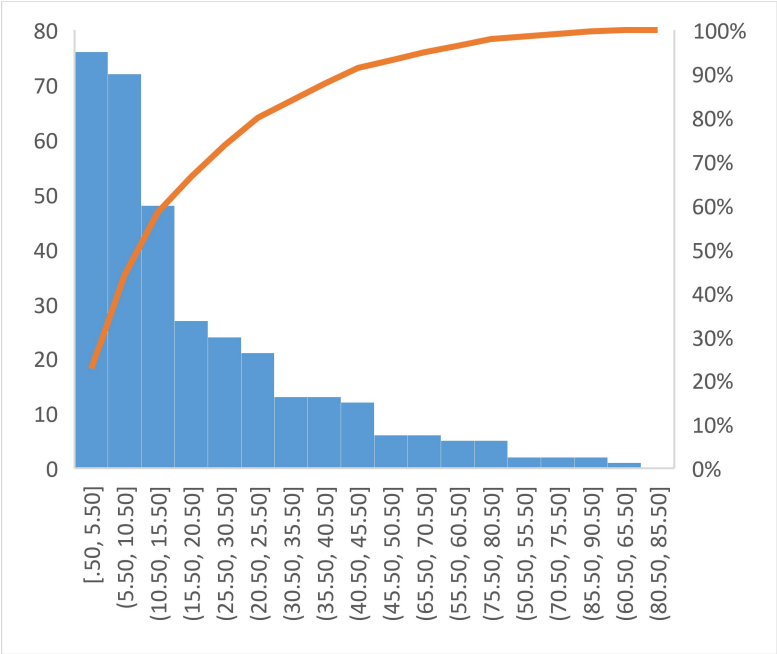

Figure 27: Histogram of the deviations, the horizontal axis defines the classes (° deviation), the left axis shows the frequency of deviations per class. The orange curve is a sum curve with scale on the right axis

It was tried to determine how many of the mean values are corresponding, but there were difficulties. The chosen method was described in chapter 3.3 and seemed reasonable, but comparing the confidence cones and the mean values does not work because the degree of scattering influences the size of the confidence cones. There are in fact datasets in which the mean values show good correspondence since they are plotting in the same confidence cone and other datasets with the mean values having a similar deviation from each other as in the first dataset and no correspondence since the confidence cones are much smaller. An example for this are 9_k1 and 9_k2 in Figure 24. Taking this into account and searching for discrepancies of the mean values, there is only one dataset, 10_k1 in Figure 26, in which the mean values and their data do not correspond. In most other datasets there is no outstanding difference between the mean values.

As mentioned in chapter 4, there are some datasets, among them 10_k1 shown in Figure 28, in which only some of the digital data do not accord with the compass data. This suggests, that a part of the accuracy problem may actually be a calibration problem. This hypothesis is also supported by 9_k1, in which the digital and the compass dataset show similar scattering, but clearly different mean values.

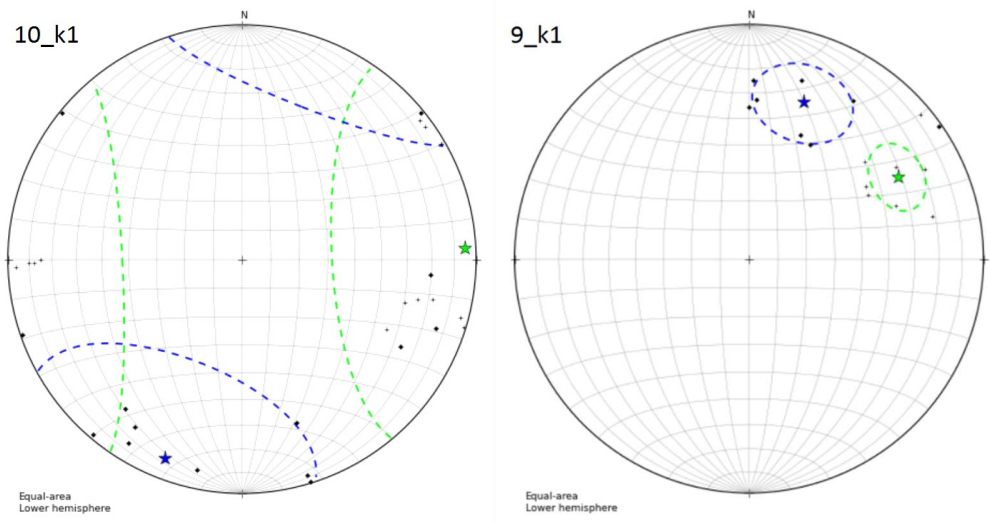

Figure 28: One of the not according datasets

To test the hypothesis of the calibration problem, deviation-time diagrams were plotted for every outcrop, one of them can be seen in Figure 29. It can be seen, that imprecise measurements seem to cluster. These clusters can be observed for every outcrop and they are every time somewhere else. If this is a calibration problem, the app calibrates all the time.

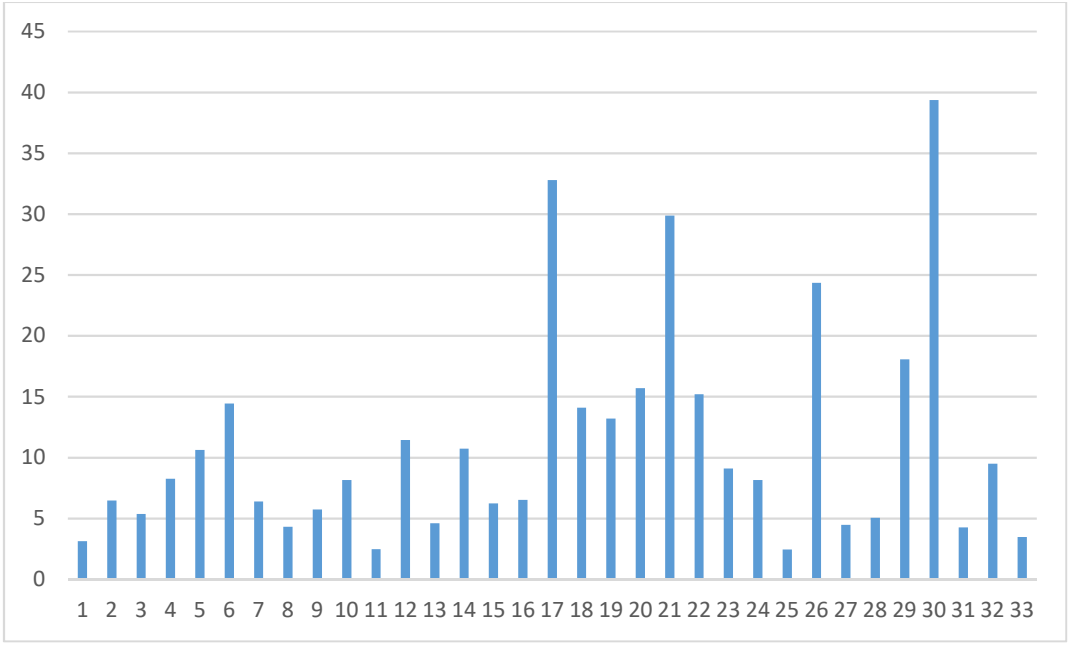

Figure 29: Deviation (vertical axis) vs number of measurement of outcrop 3

Smartphones may not be constructed to be used as geological compass, so it is possible, that their compass only works in some orientations. In Figure 30 the relation of deviations and dip angle is plotted. It can clearly be seen, that there is a trend from small deviations at small values for the dip angle to high deviations for dip angles greater than 40°.

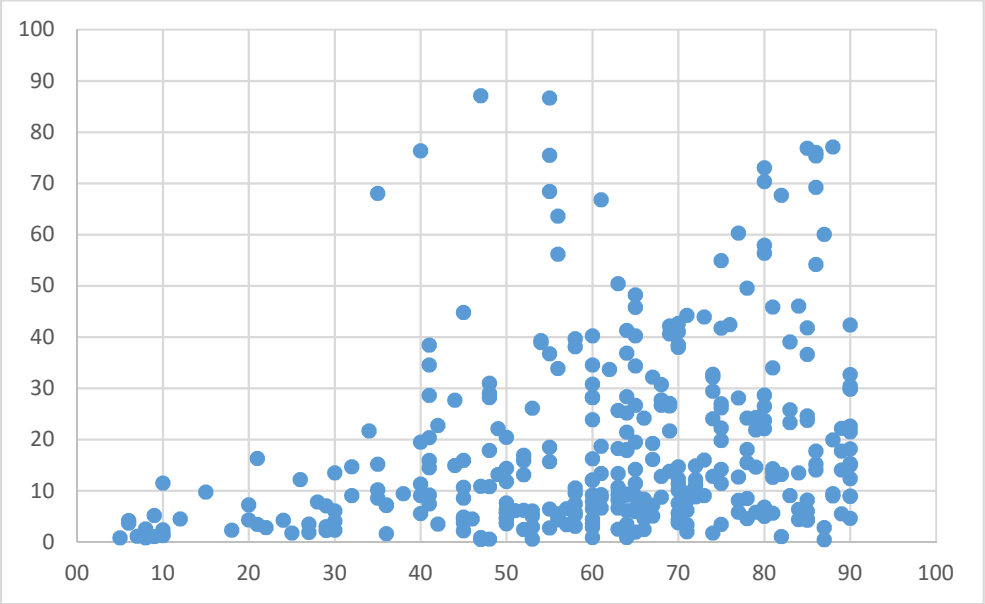

Figure 30: Dip angle (horizontal axis) vs deviation (vertical axis), units in degree

6 Conclusions

For the handling side, the digital compass is as good as promised. The measurements are fast, the energy consumption is small enough, that measurements were possible all day and the export of the data is a very nice feature – especially for large datasets. A problem with moisture and scratches could be avoided by using a waterproof smartphone cover.

For the data quality, the whole story looks a bit different. The precision of single measurements is not very good with a median of 13° deviation, this is even worse for dip angles greater than 40°. Although the precision is a problem, the accuracy is quite good. There are deviations also for the mean values, but they are in most cases acceptable and the deviations get smaller, if there are more measurements.

To conclude, modern smartphones can be used as geological compass, but it is a good advice to make some extra measurements to ensure a good accuracy.

Literature

Braitsch, O. (1956). Quantitative Auswertung einfacher Gefügediägramme. *Heidelberger Beiträge zur Mineralogie und Petrographie*, *5*(3), 210–226.

Cardozo, N., & Allmendinger, R. W. (2013). Spherical projections with OSXStereonet. *Computers & Geosciences*, *51*, 193–205.

Faryad, S. W., Melcher, F., Hoinkes, G., Puhl, J., Meisel, T., & Frank, W. (2002). Relics of eclogite facies metamorphism in the Austroalpine basement, Hochgrössen (Speik complex), Austria. *Mineralogy and Petrology*, *74*(1), 49–73.

Grohmann, C.H. and Campanha, G.A.C. (2010). OpenStereo: open source, cross-platform software for structural geology analysis. Presented at the AGU 2010 Fall Meeting, San Francisco, CA.

Melcher, F., Meisel, T., Puhl, J., & Koller, F. (2002). Petrogenesis and geotectonic setting of ultramafic rocks in the Eastern Alps: constraints from geochemistry. *Lithos*, *65*(1–2), 69–112.

Moser, M. (2016). GEOFAST Karte 132 Trofaiach. Geologische Bundesanstalt.

Neubauer, F. (1988). Bau und Entwicklungsgeschichte des Rennfeld-Mugel und des Gleinalm-Kristallins (Ostalpen). *Abhandlungen Der Geologischen Bundesanstalt*, *42*.

Neubauer, F., & Frisch, W. (1993). The Austro-Alpine Metamorphic Basement East of the Tauern Window. In P. D. J. F. von Raumer & P. D. F. Neubauer (Eds.), *Pre-Mesozoic Geology in the Alps* (pp. 515–536). Springer Berlin Heidelberg.

Neubauer, F., Frisch, W., Schmerold, R., & Schlöser, H. (1989). Metamorphosed and dismembered ophiolite suites in the basement units of the Eastern Alps. *Tectonophysics*, *164*(1), 49–62.

Sachsenhofer, R. F., Bechtel, A., Reischenbacher, D., & Weiss, A. (2003). Evolution of lacustrine systems along the Miocene Mur-Mürz fault system (Eastern Alps, Austria) and implications on source rocks in pull-apart basins. *Marine and Petroleum Geology*, *20*(2), 83–110.

Schmid, S. M., Fügenschuh, B., Kissling, E., & Schuster, R. (2004). Tectonic map and overall architecture of the Alpine orogen. *Eclogae Geol. Helv.*, (97), S.93–117.

Thalhammer, O. R., Ebner, F., Horkel, K., & Mali, H. (2010). Der Ultramafit-Komplex von Kraubath. *Journal of Alpine Geology*, *53*, 137–158.

Turner-Jones, B. (2016). Rocklogger. https://rockgecko.com/downloads/ (17.1.2017).

Appendix

Outcrops

In the following table the positions of the outcrops are written. The coordinates are in the WGS 1984 coordinate system.

Outcrop	Latitude	Longitude
1	47.28732	14.952654
2	47.295146	14.955054
3	47.289417	14.954828
4	47.290472	14.956161
5	47.292876	14.955652
6	47.293546	14.956879
7	47.293042	14.958034
8	47.287539	14.961679
9	47.288859	14.963294
10	47.290075	14.946235

Data

In the following table the measured compass data are written. The digital data was given with a precision of one decimal place by Rocklogger; but the data were rounded because it is unlikely, that the precision is really that high and the data were compared with compass data, which have at best a precision of 1°. The following abbreviations are used:

sf……. schistosity/foliation

f……fault

k……joint (from german Kluft)

L…….. Lineation

If there is a number, e.g. “k3”, this means, that there are several sets of this type, and they are numbered.

Outcrop 1		compass	compass	smartphone	smartphone
	type	dip direction	dip angle	dip direction	dip angle
1	f	007	67	4	83
2	L	282	27	286	27
3	L	274	08	276	9

4	f	258	70	262	70
5	L	331	36	343	38
6	L	328	42	330	45
7	f	272	84	268	86
8	f	270	87	270	87
9	L	186	63	181	68
10	L	186	55	187	58
11	kf	047	56	50	51
12	kf	043	63	54	53
13	sf	170	81	166	85
14	sf	172	84	178	87
15	L	241	26	221	34
16	L	260	09	290	11
17	L	270	015	283	24
18	L	265	21	296	31
19	sf	179	81	355	87
20	sf	268	60	242	65
21	sf	272	75	252	77
22	sf	267	66	242	71
23	sf	269	69	255	73
24	sf	266	68	236	69
25	L	291	60	323	62
26	L	246	56	287	58
27	L	300	64	332	65
28	k1	279	55	72	54
29	k1	274	35	61	36
30	k1	290	55	67	48
31	k1	240	47	29	44
32	L in k1	150	06	115	6
33	k2	130	60	118	66
34	k3	244	40	21	43
Outcrop 2		compass	compass	smartphone	smartphone
	type	dip direction	dip angle	dip direction	dip angle
1	sf	345	47	358	51
2	sf	347	50	357	49
3	sf	342	64	342	63
4	sf	336	68	9	68
5	sf	344	40	335	39
6	sf	335	50	351	49
7	sf	344	60	340	61
8	sf	343	60	344	57
9	h	341	90	345	88
10	h	164	68	347	85
11	h	160	85	202	89
12	h	340	78	351	67
13	L	065	50	59	53
14	L	092	70	51	59

15	k1	353	78	337	87
16	k1	000	90	331	80
17	k1	030	85	355	74
18	k1	045	77	344	82
19	k1	024	81	337	76
20	k2	150	65	151	67
21	k2	166	45	172	48
22	k2	152	70	163	75
Outcrop 3		compass	compass	smartphone	smartphone
	type	dip direction	dip angle	dip direction	dip angle
1	sf	085	58	83	61
2	sf	071	55	78	58
3	sf	082	58	83	63
4	sf	052	63	61	66
5	sf	074	58	83	65
6	sf	073	50	90	55
7	sf	068	50	74	54
8	sf	081	56	81	60
9	sf	023	50	30	53
10	sf	040	71	49	72
11	sf	040	66	41	68
12	sf	029	75	41	76
13	k1	161	45	155	47
14	k1	153	63	142	67
15	k1	149	71	144	75
16	k1	168	60	161	61
17	k1	172	74	139	79
18	k1	171	86	157	88
19	k1	172	82	344	88
20	k1	160	55	147	66
21	k1	162	90	11	81
22	k1	010	86	14	71
23	s1	166	73	175	77
24	s1	165	77	172	81
25	L1	255	10	258	8
26	f2	183	79	8	77
27	f2	005	85	2	88
28	f2	200	80	196	77
29	f2	208	64	228	67
30	f2	210	54	262	43
31	f3	021	85	20	89
32	f3	018	88	27	86
33	L	294	21	297	18
Outcrop 4		compass	compass	smartphone	smartphone
	type	dip direction	dip angle	dip direction	dip angle
1	sf2	325	75	300	84

2	sf2	326	74	338	80
3	sf2	329	73	345	78
4	sf2	332	80	259	88
5	sf2	300	65	306	67
6	sf2	312	72	297	69
7	sf2	294	85	11	86
8	sf2	324	60	11	58
9	sf2	154	90	293	80
10	sf2	306	75	284	66
11	sf2	304	65	283	66
12	sf2	310	83	316	76
13	sf2	132	90	141	89
14	sf1	161	70	157	74
15	sf1	163	74	188	72
16	sf1	150	57	147	63
17	sf1	184	81	170	81
18	sf1	168	85	175	81
19	sf1	165	81	131	75
20	sf1	162	77	149	74
21	sf1	163	90	177	84
22	sf1	162	60	176	56
23	sf1	160	66	167	69
24	sf1	150	67	179	84
25	sf1	175	88	183	83
26	sf1	180	83	157	79
27	sf1	169	75	171	72
28	sf1	150	90	2	85
29	k	044	76	85	88
30	k	055	74	56	76
31	k	058	50	55	53
32	k	066	61	61	66
33	k	072	53	67	58
34	k	008	66	6	70
35	k	008	65	354	71
36	k	020	61	21	70
37	k	011	64	13	67
38	k	072	64	75	69
39	k	054	60	59	62
40	k	040	64	50	66
41	k	036	58	41	62
42	k	038	51	44	55
43	k	045	46	44	51
44	k	030	60	29	60
45	k	018	50	17	54
46	f	308	84	123	83
47	f	130	90	135	76
Outcrop 5		compass	compass	smartphone	smartphone

	type	dip direction	dip angle	dip direction	dip angle
1	sf1	252	55	341	51
2	sf1	295	41	237	45
3	sf1	260	50	287	44
4	sf1	253	55	299	51
5	sf1	248	45	318	38
6	sf1	230	60	271	53
7	sf1	248	60	279	46
8	sf1	238	61	323	46
9	sf1	250	48	251	37
10	sf1	265	58	254	56
11	sf1	244	41	230	27
12	sf1	245	68	251	56
13	sf1	246	63	225	44
14	sf1	255	70	263	68
15	sf1	240	70	245	70
16	sf1	241	65	293	58
17	sf1	260	69	288	63
18	sf1	074	86	330	89
19	sf1	075	87	315	87
20	sf2	351	63	351	66
21	sf2	348	67	334	81
22	sf2	001	71	358	72
23	sf2	002	64	10	70
24	sf2	022	57	25	59
25	sf2	014	63	20	70
26	sf2	346	53	348	58
27	sf2	356	71	357	73
28	sf2	338	68	332	75
29	k	081	27	80	24
30	k	090	47	90	47
31	k	099	47	98	47
32	k	080	29	82	32
33	k	070	52	75	47
34	f	312	53	308	54
35	f	308	45	300	52
36	f	338	45	341	45
37	f	328	48	329	48
Outcrop 6		compass	compass	smartphone	smartphone
	type	dip direction	dip angle	dip direction	dip angle
1	sf	007	41	60	42
2	sf	001	34	41	32
3	sf	312	10	318	11
4	sf	286	22	291	24
5	sf	295	18	287	18
6	sf	323	29	310	31
7	sf	286	20	294	27

8	sf	326	20	331	24
9	sf	313	07	316	6
10	sf	296	12	307	16
11	sf	306	36	305	38
12	sf	305	36	294	39
13	sf	303	40	301	49
14	sf	300	35	288	39
15	sf	316	52	303	60
16	sf	304	41	293	47
17	k1	102	72	93	65
18	k1	105	60	69	52
19	k1	104	72	116	68
20	k1	082	61	91	58
21	k1	081	80	80	74
22	k1	086	80	61	68
23	k2	016	70	196	72
24	k2	024	69	181	75
25	k2	025	70	175	79
26	k2	167	90	2	86
27	k2	152	90	350	89
28	k2	162	90	4	84
29	st	006	65	36	61
30	st	357	83	32	63
31	f	008	74	178	75
32	f	023	65	188	69
33	f	043	80	153	88
34	f	026	56	204	60
35	f	056	77	223	78
36	f	033	74	233	84
Outcrop 7		compass	compass	smartphone	smartphone
	type	dip direction	dip angle	dip direction	dip angle
1	sf	330	44	12	35
2	sf	002	40	351	30
3	sf	332	30	304	27
4	sf	328	35	354	28
5	sf	003	32	31	27
6	sf	330	40	359	29
7	sf	019	38	21	29
8	sf	350	32	4	26
9	sf	010	45	24	40
10	k2	170	78	170	73
11	k2	172	78	163	79
12	k2	169	82	170	82
13	k2	171	84	217	86
14	k1	267	75	280	81
15	k1	090	83	115	74
16	k1	100	89	87	85

17	k1	072	85	97	81
18	k1	270	78	109	87
19	k1	272	80	119	89
20	k1	105	90	95	83
21	k1	112	80	90	73
22	sf	269	08	274	7
23	sf	019	10	287	5
24	f1	163	50	158	52
25	f1	171	56	165	57
26	f1	149	52	147	50
27	f1	162	53	162	54
28	f2	241	65	229	67
29	f2	251	41	240	39
30	f2	247	44	261	55
31	L	185	30	177	29
32	L	175	35	178	25
Outcrop 8		compass	compass	smartphone	smartphone
	type	dip direction	dip angle	dip direction	dip angle
1	sf	095	77	101	77
2	sf	102	67	106	64
3	sf	088	65	98	64
4	sf	106	71	103	80
5	sf	098	79	104	77
6	sf	132	45	136	48
7	sf	119	50	123	53
8	sf	110	79	132	80
9	sf	113	67	119	72
10	sf	094	60	97	67
11	sf	084	70	91	81
12	sf	085	85	109	87
13	sf	100	80	104	86
14	L1	109	64	81	63
15	L1	152	58	143	59
16	L1	137	56	135	51
17	L1	113	70	97	71
18	L1	140	65	136	71
19	L2	187	05	184	6
20	L2	212	10	205	10
21	L2	204	08	193	10
22	L2	002	06	6	2
23	k2	110	09	109	10
24	k2	167	30	155	30
25	k2	142	24	139	28
26	k2	206	52	186	47
27	k2	141	28	153	33
28	k1	003	55	24	60
29	k1	009	60	19	57

30	k1	019	42	17	65
31	k1	019	61	30	44
32	k1	358	48	29	65
33	k1	357	48	18	56
34	k1	016	82	129	89
35	k1	022	45	34	58
36	k1	048	41	62	52
Outcrop 9		compass	compass	smartphone	smartphone
	type	dip direction	dip angle	dip direction	dip angle
1	sf	358	64	334	65
2	sf	356	64	336	62
3	sf	358	65	315	71
4	sf	183	89	165	86
5	sf	175	87	178	87
6	sf	178	90	349	87
7	sf	007	75	339	72
8	sf	353	81	339	82
9	sf	175	71	338	68
10	sf	002	79	348	75
11	sf	013	64	332	63
12	sf	358	70	347	69
13	sf	172	90	202	89
14	sf	006	60	348	62
15	k1	238	49	208	46
16	k1	238	63	182	65
17	k1	257	69	213	70
18	k1	230	54	183	57
19	k1	250	56	180	54
20	k1	243	73	197	68
21	k1	242	48	203	48
22	k1	230	85	235	88
23	k2	120	49	104	52
24	k2	160	69	131	70
25	k2	155	75	111	70
26	k2	305	89	310	87
27	k2	124	52	105	59
28	k2	147	53	115	57
29	L1	088	29	87	31
30	L1	090	25	87	26
31	L1	075	30	77	28
Outcrop 10		compass	compass	smartphone	smartphone
	type	dip direction	dip angle	dip direction	dip angle
1	sf	175	62	138	68
2	sf	145	70	189	60
3	sf	168	65	206	64
4	sf	167	80	226	72

5	sf	164	48	203	35
6	sf	167	41	198	31
7	k1	089	80	32	81
8	k1	090	75	33	74
9	k2	215	58	172	65
10	k3	359	41	38	49
11	sf	171	69	150	77
12	sf	171	63	151	67
13	k1	285	61	299	66
14	k1	283	66	275	70
15	k1	296	58	342	63
16	k1	287	89	129	89
17	k1	285	86	231	88
18	k1	282	72	290	77
19	k1	232	86	343	89
20	k1	240	88	343	86
21	k1	240	88	40	88
22	k1	234	86	71	89
23	k1	089	78	38	70
24	k1	088	86	12	81
25	sf	003	64	317	64
26	sf	003	90	343	83
27	sf	060	80	36	78